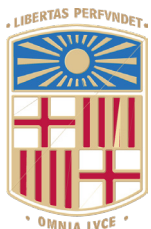


## Book of Tutorials and Abstracts

---



European Microbeam Analysis Society

---

# EMAS 2025

18th  
EUROPEAN WORKSHOP

on

# MODERN DEVELOPMENTS AND APPLICATIONS IN MICROBEAM ANALYSIS

11 to 15 May 2025  
at the  
TecnoCampus  
Mataró (Barcelona), Spain

---

Organized in collaboration with the  
Universitat de Barcelona, Spain

---

*EMAS*

European Microbeam Analysis Society eV

[www.microbeamanalysis.eu/](http://www.microbeamanalysis.eu/)

This volume is published by:

European Microbeam Analysis Society eV (EMAS)

EMAS Secretariat

c/o Eidgenössische Technische Hochschule, Institut für Geochemie und Petrologie

Clausiusstrasse 25

8092 Zürich

Switzerland

© 2025 *EMAS* and authors

ISBN 978 90 8227 6985

NUR code: 972 – Materials Science

All rights reserved. No part of this publication may be reproduced, stored in a retrieval system, or transmitted in any form or by any means, electronic, mechanical, by photocopying, recording or otherwise, without the prior written permission of *EMAS* and the authors of the individual contributions.



## **ICONIC INSTRUMENTS FOR ART: COMBINED ANALYSIS TECHNIQUES IN CULTURAL HERITAGE**

**Michele Gironda, R. Tagle, M. Gerken, Y. Yang, M. Abratis and N.M. Kelly**

Bruker Nano Analytics  
Am Studio 2D, 12489 Berlin, Germany  
e-mail: [michele.gironda@bruker.com](mailto:michele.gironda@bruker.com)

Michele Gironda is the Business Development Director at Bruker AXS, overseeing global activities related to Art & Conservation and Clean Energy. In his activity he collaborates closely with prominent museums, institutes, and university departments to promote new instruments specifically tailored for art studies. His work includes significant measurement campaigns on art objects, resulting in over 32 scientific publications throughout his career.

Prior to joining Bruker, Michele was the Director of Sales and Marketing at XGLab S.R.L., which was later acquired by Bruker.

He holds a MSc degree in Engineering from Politecnico di Milano (Italy) and Universitat Politècnica de Catalunya (Spain).

## *1. ABSTRACT*

Elemental investigation of solid materials either using electron or photon excitation was first described more than 70 years ago [1-7]. Since then, techniques have progressively evolved from niche applications to become common and indispensable in materials analysis across industrial and research applications. Application flexibility, such as the ability to study well-defined, small sample areas or larger areas of non-homogenous materials, collection of large data sets in a short time, access to major and trace element information, and the capability to conduct non-destructive sample analysis, meant these techniques were quickly adopted by Heritage and Conservation scientists and have become core techniques used for Cultural Heritage object investigation. Ongoing technological developments that have led to improved excitation sources, enhanced detection sensitivities and faster signal processing capabilities, and advanced algorithms that allow more accurate elemental quantification, have allowed significant improvement in instrument performance and data quality, making microanalysis a standard analytical tool in Cultural Heritage studies. In this paper the utility of micro-XRF spectroscopy ( $\mu$ -XRF) and scanning electron microscopy (SEM) for the study of cultural important objects will be presented using examples of measurements on paintings, metallic and ceramic objects, and on historical photographs. The applications will demonstrate how X-ray and electron beam techniques differ but may be used in a complementary manner to access the rich detail of these objects.

## *2. INTRODUCTION*

The most universal and best-known techniques for analysis of cultural heritage objects include optical and electron microscopy (including SEM-energy-dispersive X-ray spectrometry (SEM-EDS) and electron probe microanalysis (EPMA)), X-ray diffractometry (XRD), and X-ray fluorescence (XRF), as well as vibrational spectroscopy methods such as (FT-)IR and Raman spectroscopy. Together these techniques combine the possibility to magnify features, visualise compositional variations, characterise crystallographic properties, and determine major and trace element composition of a variety of samples and materials of inorganic and organic nature [8]. Of these, the latter is perhaps the most important key to understanding the full breadth of an object's history, from the materials and the methods used in production to events that caused alteration to the object such as degradation and/or restoration.

With the breadth of options available to modern Cultural Heritage Science, choice of method may be defined by object characteristics and specific analytical considerations that arise when approaching the study or conservation of that object. Considerations include:

- Location of an object, such as in a museum, laboratory, church, or temple, which impacts how a measurement may be collected and time available for such measurements.
- The sample to be analysed – a painting, a metal object such as coins, armour, or weapons, a sculpture, or ancient documents produced on paper or parchment.

- Analytical question. A study may need exact (quantified) compositions or comparative (relative) compositions. The study may need to evaluate a multilayer structure such as glazes or even identifying a possible underpainting or pentimenti. A more recent trend is to determine the possible presence of a contamination in a collection, such as arsenic used as a pesticide to preserve historical books.

Consideration should also be given to the scales of information across analytical techniques. A natural tendency is to attempt to access compositional information at the highest resolution and most detail accessible. SEM represents one of the few easily accessed techniques that provides analysis at the finest scales – micrometre to sub-micrometre scale imaging and elemental characterisation. At these scales, SEM analysis also provides the means to ground truth interpretations made from other techniques that may not afford such high spatial resolution. However, techniques such as SEM analysis are by nature invasive. Samples are limited to those that fit within an SEM chamber and can be placed under vacuum. In many cases this requires pieces of an object or painting to be cut, mounted in epoxy resin and polished to a flat surface, and depending on circumstance coated to be conductive. Many SEMs may run in low vacuum mode, allowing measurements in the absence of conductive coatings, but with a resulting reduction in spatial resolution.

Cultural heritage objects, from the oldest archaeological artefacts to very recent modern works of art, are precious. Therefore, any workflow will reflect the desire for any analysis to be non-invasive wherever possible. Where invasive measurements are absolutely necessary all attempts are made to limit any additional impact to the object through sub-sampling or sample preparation. In addition, the delicacy of many objects due to age and/or value means that sample preparation is complicated and time-consuming leading to a natural tendency to “optimise” the number of samples studied. While well intentioned, this increases the chance of analytical misinterpretation due to non-representative sampling. Therefore, use of complementary analytical techniques that require minimal or no sample preparation are employed to optimise the location and number of samples processed. Workflows will, therefore, typically start at broader scale non-invasive characterisation to ensure any invasive sampling occurs only where necessary, and where the resulting SEM data will have maximum knowledge impact.

X-ray fluorescence analysis, through application of portable XRF devices for localised spot analysis or large-area scanning  $\mu$ -XRF for the collection of elemental maps, allows non-destructive investigation of objects and collection of data that provides important information not feasible using electron beam analysis, and also the critical context for effective representative or feature sampling.

### *3. COMPARISON OF ANALYTICAL TECHNIQUES*

Compositional analysis by electron beam (e.g., SEM, EPMA) and in situ X-ray beam-based techniques (e.g.,  $\mu$ -XRF) show certain in-principle similarities – both rely on the generation of fluorescence X-rays due to the interaction of electrons or primary photons with atoms within a sample and employ EDS spectrometers for the detection of the X-ray signals [9]. However, it is in their differences that the greatest analytical potential is offered.

One of the main differences is in the spatial resolution of the primary beam. In electron excitation, the electron beam can be focussed down to a few nanometres and the interaction volume (determined by the mean free path of the electrons within the sample) can be efficiently “adapted” to the application by adjusting the electron acceleration voltage. This provides an advantage to the investigation of very fine detail in samples by limiting mixed signals. In comparison, the focussing options for photons are limited and rely on collimators to generate narrower beams, which may compromise the intensity of primary photons reach the sample and may limit the working distance. With more advanced systems, small spot sizes are achieved using advanced optics such as polycapillary lenses where beams may be focused to  $< 10 \mu\text{m}$  without significant loss of primary intensity.

Additionally, the depth of penetration of photons into a sample is greater than for electrons, while the options for controlling the penetration depth and therefore the interaction volume of photons in the samples are limited [10-11]. For XRF, interaction volume is a combination of the beam width and the emission depth of fluorescence X-rays, which will be shallower than penetration depth and determined by the matrix density and energy of the individual X-ray lines (that is, deeper for higher energy fluorescence X-rays such as Pb-L $\alpha$  at 10.55 keV, compared with lower energy fluorescence X-rays such as Pb-M $\alpha$  at 2.34 keV) [12]. However, this deeper emission depth may become an advantage in analysis of layered objects due to the ability to observe features below the surface, and the smaller interaction volume of an electron beam a limiting factor.

Although not always yielding to optimal results for characterisation of the finest detail, X-ray fluorescence analysis has an advantage of being a non-invasive technique where the sample can be analysed without prior preparation. In addition, the higher signal/noise ratio for XRF allows for much lower limits of detection, where the absence of elastic scattering results in lower backgrounds (Fig. 1). Combined these features make the XRF instrument extremely accessible for fast initial assessment of sample compositions. On the other hand, for SEM measurement the sample must fit in the analytical chamber and the ideal sample for an electron-based excitation should be conductive. In principle, any sample can be measured directly and without any sample preparation, including liquids, solids, or powders.

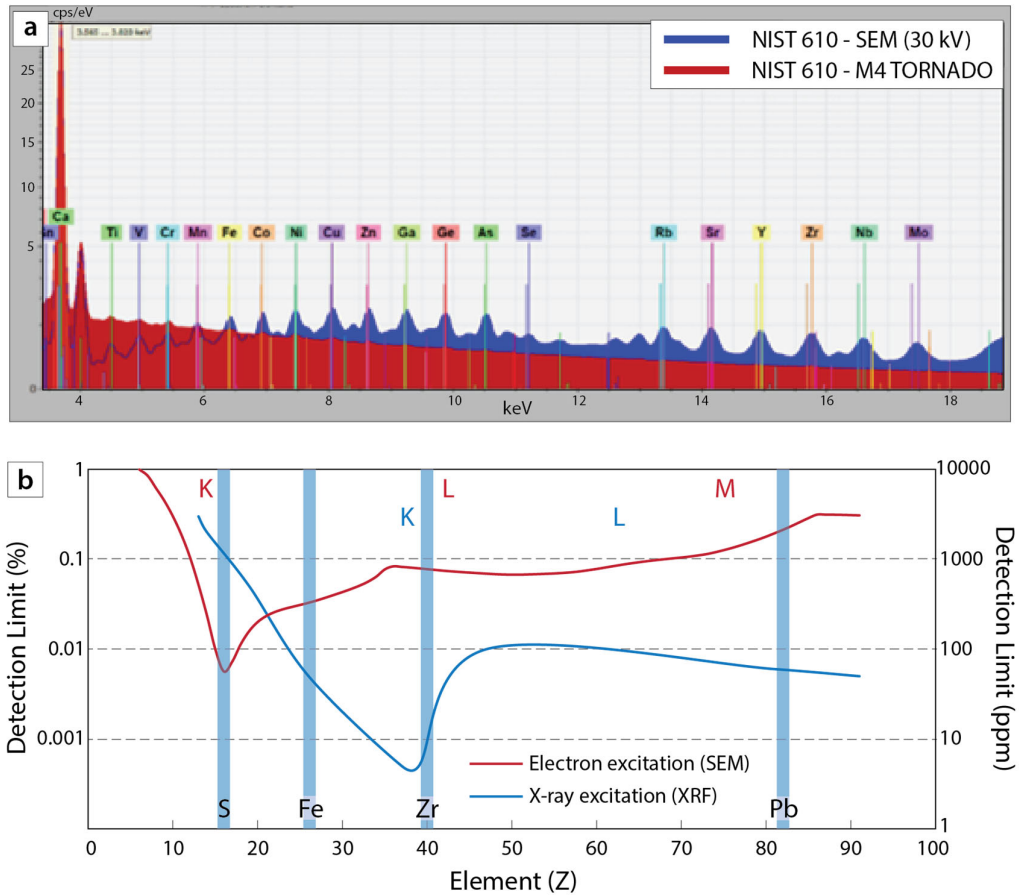


Figure 1. Differences in limits of detection (LOD) between photon and electron excitation. a) EDS spectra collected on the NIST 610 standard emphasising the higher excitation efficiency of photons and greater signal to noise ratio in the energy region above 6 keV. b) Relative differences in LOD.

An important contrast in analytical performance between SEM and XRF analysis is in excitation efficiency across the range of elements (see example in Fig. 1a). The lower energy of electron beams limits excitation of higher energy X-rays like those characteristics of many trace elements of interest to cultural heritage studies. In contrast, the ionisation cross-section for most elements is higher for photons providing efficient excitation of higher energy X-ray lines. This very feature leads to limited low energy excitation by X-ray beams, where SEM-EDS analysis has a clear advantage. Light element performance of SEM systems is further enhanced by the ability to measure under vacuum, improving low-energy X-ray transmission from the sample surface to the detector. For open beam XRF systems, light elements are typically attenuated by interactions with the atmosphere. Whereas the possible use of light-element windows has progressively removed the historical transmittance penalty present in XRF systems (where 8  $\mu\text{m}$  or 12.5  $\mu\text{m}$  thick beryllium windows were typically used), we still see a clear difference in the excitation efficiency between XRF and SEM-EDS. In an ideal intersection between both worlds, it is now

possible to install a  $\mu$ -XRF source on an SEM column for analyses across the entire X-ray spectrum, combining fine-focus / small volume analysis of an electron beam with depth / layer analysis of an X-ray source, all under the same atmosphere.

#### 4. APPLICATION EXAMPLES

##### 4.1. Paintings

The first application examples will focus on paintings across different media and will be used to contrast the analytical approaches and data outcomes of open-beam large-area scanning  $\mu$ -XRF of entire paintings, compared with focussed SEM-EDS analysis of a sub-sample of paint. The application will demonstrate the combined benefits of integrating both techniques in the study of paintings and wall art.

The first example is a measurement conducted at the Museo Nacional de Arte Antigua (MNAA) in Lisbon, where the St. Vincent Panels (attributed to Nuno Gonçalves) were scanned. In this case, it was required to bring the measurement system on-site as it was not possible to move the panels due to their delicate state and high value in Portugal. The goal of the measurements was to study the status and previous restoration in the frame of a new restoration campaign. Despite the large areas that needed to be scanned within a limited time, the utility of large-area  $\mu$ -XRF scanners made this possible.

The instrument employed was the CRONO non-contact  $\mu$ -XRF Scanning Spectrometer (Bruker Nano GmbH, Berlin), configured with a 10 W X-ray tube with Rh anode and  $50\text{ mm}^2$  active area silicon drift detector (SDD), operated at 50 kV accelerating voltage, 200  $\mu\text{A}$  beam current, and a stage speed of 10 mm/s. This scanner, through its ability to cover areas up to  $60\text{ cm} \times 45\text{ cm}$  in a single scan was instrumental in collecting large but detailed overview maps quickly (see Figs. 2a and 2b). The technique was able to identify the original pigments used (linked to the presence of elements such as Hg, Ca, Pb, Cu; Fig. 2b). The mapping was also able to detect extensive areas of previous restoration activities through the identification of anachronistic (non-period) pigments evident through their characteristic elements (Ti, Cr, Zn; Fig. 2c).

In the second example we leveraged the capability of XRF to examine art objects and explore for the presence of pigment layers not visible to the naked eye. This activity took place at Villa Borghese in Rome, focussing on Raphael's masterpiece "La Deposizione Baglioni." XRF scanning was also conducted using the CRONO  $\mu$ -XRF Scanning Spectrometer, at conditions identical to those detailed above. Positioning of the CRONO during one of the scans is presented in Fig. 3a.



Figure 2. Element maps of the “St Vicent Panels”, (attributed to Nuno Gonçalves) acquired at the Museo Nacional de Arte Antigua. a) Visual image of select panels from the collection, including locations of two maps collected. b) Elemental map illustrating distribution of original pigments in the painting. c) Elemental map showing overpaint (earlier restoration) using non-period pigments.

During this examination, a pentimento (original elements of a painting that were subsequently painted over by the artist) was identified. In this example the Sr-K $\alpha$  X-ray line, which was excited through interaction of the deeply penetrating primary X-rays, had sufficient energy to pass through the overlying layers of pigment. In this case, Sr originates from gypsum, used in the first preparation layer and outline of figures, some of which were further elaborated in the final version of the painting. This preparation layer remained differently exposed in the area where a figure was initially planned to be painted but was later covered by the landscape (compare Fig. 3b with Fig. 3c) [13].

While the large area scans provide invaluable information over broad portions of a painting, when the layering structure becomes more complex, or the level of detail falls below the resolution of the X-ray beam, we need to employ SEM analysis to confirm and extend the findings accessible with XRF. In collaboration with Dr. Marta Ghirardello and the ArtIS Laboratory at Politecnico di Milano, the opportunity was provided to analyse fragments from the wall painting of "The Last Supper" (Fig. 4a) by Leonardo da Vinci, a masterpiece of Renaissance art renowned for its artistic brilliance and experimental technique. In this study, we re-examined



Figure 3. Illustration of the mobile capability of scanning  $\mu$ -XRF devices during a measurement campaign at the Villa Borghese, Rome. a) CRONO scanning XRF positioned for measurements in front of Raphael's "La Deposizione Baglioni". b) Visual image of a targeted area of the painting focusing on a region of landscape. (c) Elemental map (Sr) reveal the presence of a hidden figure (below arrow) now obscured by the landscape.

a cross-section micro-sample carefully removed from the mural. This cross-section was mounted in epoxy and carefully polished to reveal a planar surface (Fig. 4b) and coated with carbon. Elemental maps were collected using an annular EDS detector (XFlash® FlatQUAD, Bruker Nano GmbH, Berlin), which provides improved solid angle and much higher count intensity compared with conventional EDS. This configuration allows maps to be collected at significantly lower beam currents, limiting beam damage to sensitive samples, while still achieving count rates required for rapid mapping. The objective of mapping was to gain insights into the chemical composition of pigments used in different layers of the mural, shedding light on Leonardo's development of exceptional and innovative wall painting techniques.

The resolution afforded by the SEM-EDS mapping analysis of the cross-section revealed the main components of pigments used in each layer of the painting, even amidst complex mixtures (Figs 4c to 4e). Interestingly, evidence suggests that Leonardo repeatedly adapted the final painting, as indicated by overworked areas with similar chemical compositions.

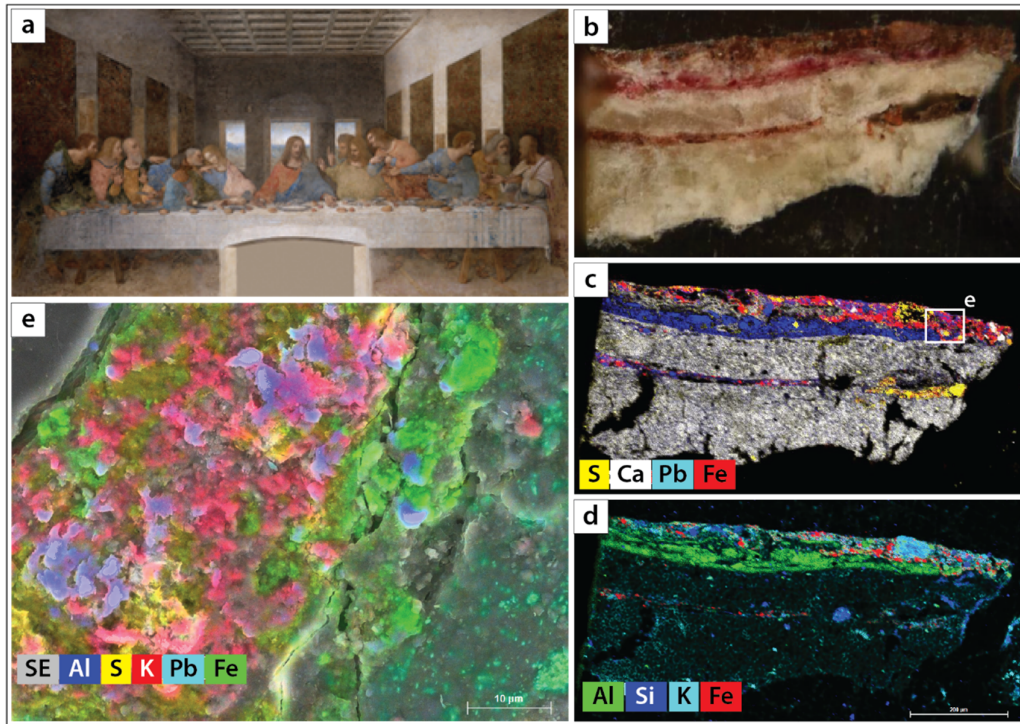


Figure 4. Scanning electron microscope investigation of a paint cross-section extracted from “The Last Supper”, Leonardo da Vinci. a) Visual image of The Last Supper. b) Optical microscope image of the cross-section, taken from the painting and mounted in epoxy resin. c and d) Elemental maps of the entire cross-section illustrating complex mixed components within and between paint layers. e) High magnification image of a small portion of the cross-section collected using the XFlash® FLATQuad annular EDS detector.

#### 4.2. Metals and other objects

Metal objects are excellent candidates for elemental analysis by XRF and SEM. The characteristic elements of their alloy composition are detectable with good efficiency. In addition, the high density of the material results in a shallow information depth, allowing for infinite thickness criteria to be established for XRF measurements (sample thickness is greater than the emission depth of X-rays being measured) even in relatively small and/or thin objects. In this case a fundamental parameter calibration may be applied, supported by type standardisation using certified reference materials, resulting in quantification with high accuracy.

An example presented here is from the study of Stater gold coins. A stater was a coin used in ancient Greece and then used in other parts of Europe and provide important insights into metallurgy practices from these eras. The hypothesis of an advanced production process was tested by examining the typical compositions of multiple coins and comparing that to a now established understanding of the relationships between proportions of Au, Cu, and Ag, and the colour of the resulting alloy (Fig. 5). Point measurements by micro-XRF conducted using the M4 TORNADO  $\mu$ -XRF Spectrometer (Bruker Nano GmbH, Berlin) with a  $< 20 \mu\text{m}$  spot size,

allow precise measurement of coin composition while avoiding non-representative areas such as tarnish or other patina on the coin surface (see XRF map in Fig. 5). Compositions revealed by this analysis positioned the relative concentrations of Au, Cu, and Ag at the exact point where it was possible to produce a yellow coin while using the minimum possible amount of gold [14].

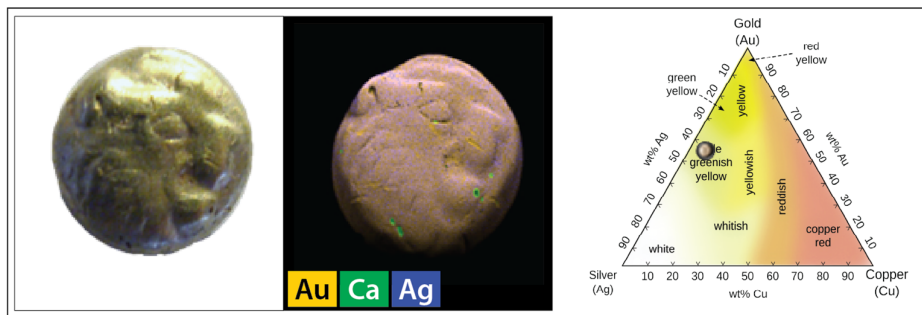


Figure 5. Stater gold coin. a) Visual image. b) Elemental map collected using M4 TORNADO  $\mu$ -XRF. c) Ternary compositional plot (Au-Ag-Cu) showing the average composition of the coin mapped relative to alloy colour.

A different approach may be required when analysing metal samples with inhomogeneities due to colouring, recasting, addition of decorations, and the presence of inclusions that offer a specific fingerprint related to material provenance but are at the scale below that of a  $\mu$ -XRF beam. In this example, a sample of a brass chest plate from Roman scale armour found at the Mušov site in the Czech Republic (provided by the Institute of Archaeology of the Czech Academy of Sciences, Brno; Fig. 6a), contains Sn- and Pb-rich microstructures containing trace levels of other impurities (Ag and Se, respectively) that provide an important means to provenance artifacts. For standard SEM-EDS measurements detection of Ag and Se at trace levels presents a challenge due to the background levels in the region of their X-ray lines. However, using a wavelength-dispersive X-ray spectrometer (WDS; XSense®, Bruker Nano GmbH, Berlin), which not only provides improved peak separation but has lower background in particular regions of the spectrum. When used on the same column this provides an ideal workflow where initial SEM-EDS mapping may be used to locate Sn- and Pb-rich domains (Fig. 6b) followed by target WDS point measurements. An example of the energy region covering Se-L $\alpha$  comparing resolution differences between EDS and WDS spectra is provided in Fig. 6c.

#### 4.3 Historical photography

Elemental analysis techniques have been important to the study of historical photographs to better understand the chemical processes used to create these objects, but also their alteration since production. Over time, the chemical composition of the materials used to generate a photographic image may change structure or react with other substances, potentially altering

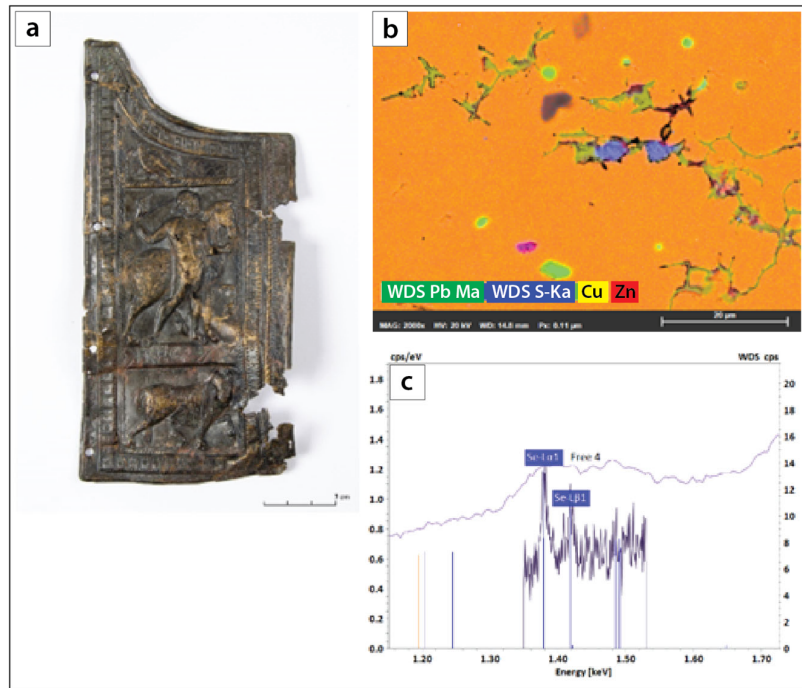


Figure 6. Illustration of the benefits from integrated EDS-WDS analysis by SEM. a) Chest plate from Roman scale armour. b) Combined EDS-WDS elemental map of a sub-sample from the chest plate showing defects in the metal rich in Pb and Zn. c) Extracted portion of the energy spectrum from a point analysis of a Pb-rich inclusion showing the increased ability to resolve the Se peak in a WDS spectrum.

the optical properties and causing the image to fade partially or completely. While some conservation processes may slow or halt degradation of photographic objects, one goal is to recover lost images.

Highly-resolved micro-XRF elemental mapping is one approach that may support the reconstruction of such images, as the elements of interest present in the original material (e.g., Ag or Hg) may be preserved in their exact locations even if the compound they now occur in has led to visual image loss. In some cases this allows for a complete reconstruction with a very high level of detail. In the example presented in Fig. 7a, a silver gelatin print depicting two children (attribution uncertain, but acquired from a reseller in the Republic of Georgia) has an area of fading of the original image in the upper left quadrant, obscuring detail of the older child's face and hat.  $\mu$ -XRF elemental mapping (M4 TORNADO  $\mu$ -XRF Spectrometer, Bruker Nano GmbH, Berlin) has characterised the elemental distribution within the photograph. The maps not only reveal the real image in great detail through the unaltered distribution of Ag (Fig. 7b), but the correlation between elevated iodine concentration and areas of fading in the visual image (compare Figs. 7a and 7c) suggest that the original unexposed photosensitive AgBr and AgI salts were not adequately removed during production and continued to react to light with time.

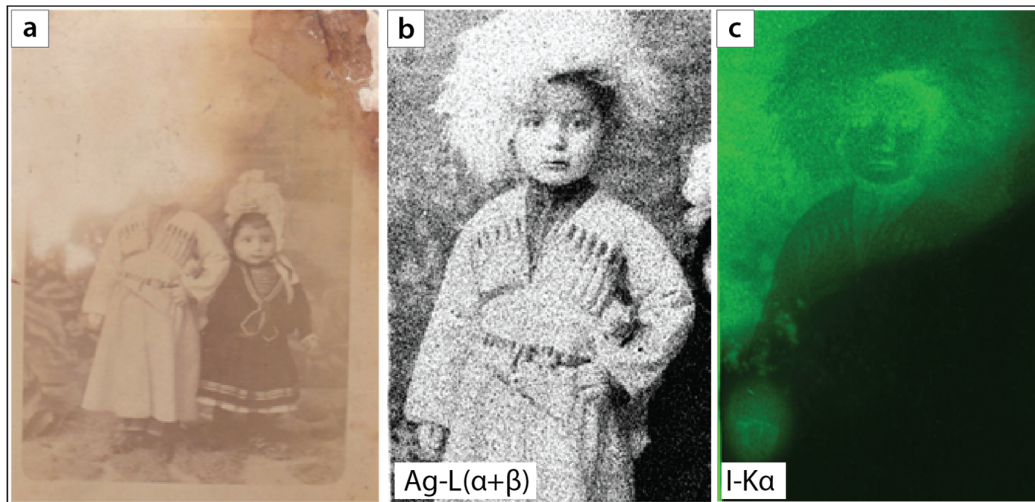


Figure 7.  $\mu$ -XRF elemental mapping of silver gelatin photographs. a) Historical photograph showing intense fading and loss of the originally recorded image (upper left quadrant). b) Elemental map (Ag-L $\alpha$ +L $\beta$ ), which records the original captured image preserved despite photo degradation. c) Iodine elemental map (I-K $\alpha$ ) illustrating the correspondence between relatively higher iodine concentrations and regions of fading.

A second example, kindly shared by Drs. Edward Vicenzi and Thomas Lam (Smithsonian Institution, Washington DC), delves deeper into an older photographic process and investigates the working techniques of early daguerreotypists, particularly those from the formative years of the process between 1839 and 1842. In the daguerreotype process, a layer of highly polished silver was applied to a copper plate, and a photosensitive layer produced through exposure to iodine and bromine fumes. While the best photographic plates were produced in France, these early photographers often had to create images on inferior plate stock due to the lack of access to French plates, which were regulated by the government to contain pure silver.

Surface imaging of photographic plates by SEM (Fig. 8a) has revealed much detail on the chemical distribution of the reactive layer. However, to investigate layers below the immediate surface is limited by the interaction volume of the electron beam. Here a SEM equipped with an on-column  $\mu$ -XRF source (XTrace® micro-XRF, Bruker GMBH, Berlin) was used to develop a non-destructive method for quantitative estimates of internal layer thickness within early photographs. Initial comparative data (Fig. 8b) collected using SEM-based  $\mu$ -XRF on historical plates and modern experimental plates with known layer thicknesses has shown significant promise for future investigations [15].

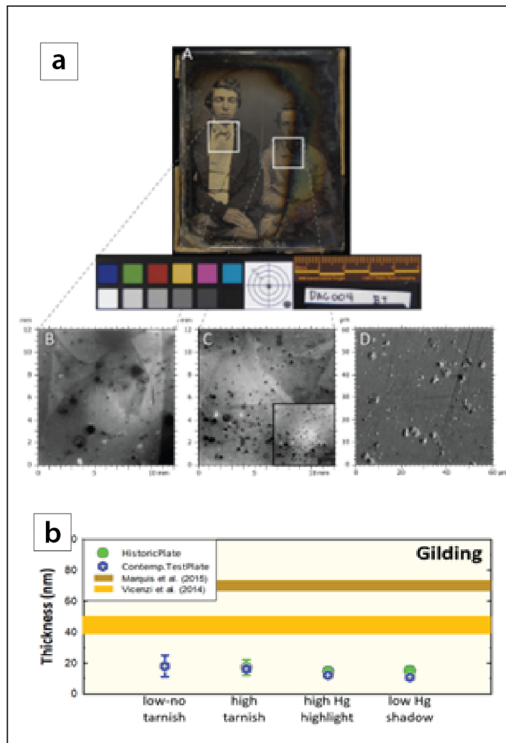


Figure 8. Layer analysis experiments on daguerreotype photographic plates using a SEM-mounted  $\mu$ -XRF source. a) Daguerreotype with surface imaging by SEM. b) Preliminary results of  $\mu$ -XRF layer analysis of experimentally produced and historical daguerreotype plates.

#### 4.4 Ceramics

Ceramic is a term that may have many meanings, but in the field of cultural heritage describes a very diverse range of materials that include anything from earthenware to high art porcelains. Those studying ceramic objects may be interested in the compositions and sources of raw materials to trace the origins of artefacts, and understanding the technologies and methods used to manufacture ceramics and how they changed through time.

In the first example, we examined an unglazed biscuit porcelain piece sculpture the provenance of which was questioned. These measurements were performed in collaboration with Prof. Phillippe Colombe (CNRS - Sorbonne Université), Mareike Gerken (Bruker Nano), and Viviane Mesqui at the Sèvres Museum, Paris. For comparison purposes, similar objects from the manufacturing sites of Sèvres and Limoges were examined. In the biscuit technique the porcelain remains perfectly exposed, which combined with their relatively homogeneous composition made these samples ideal for characterising the body material due to the absence of attenuating preparatory layers and glazes. Measurements were conducted with an ELIO scanning XRF instrument (Bruker Nano GmbH, Berlin), which is equipped with a 4 W X-ray tube with Rh anode focussed to a 1 mm X-ray spot using a fine-focus collimator, with X-rays

detected by a 17 mm<sup>2</sup> active area SDD. The ratios of intensity of typical trace elements (Y, Rb, Sr, Zr) from spot measurements provides an accurate fingerprint for determining material provenance. In this case (Fig. 9), it was relatively straightforward to associate the provenance of an unknown sculpture with Sèvres manufacture [16].



Figure 9. a) Sculpture produced using the biscuit technique, Sèvres Museum, Paris. b) Small-spot XRF point analysis of the ceramic sculpture compared to the composition of known manufacturing sources.

Highly inhomogeneous ceramics, such as earthenware, which may be produced by firing of a combination of impure clays and temper (additives such as mineral grains used to provide stability), or organic materials that act as a flux during firing, present a greater challenge for investigation. A common approach for general characterization is the use of portable XRF devices (pXRF), which provide a fast, non-destructive bulk chemical measurement of the ceramic in the vicinity of the spot (between 3 - 8 mm diameter). Additional detail on the ceramic structure and composition can be revealed by the use of  $\mu$ -XRF but is still limited by spot size and interaction volumes. Where sample preparation is possible, SEM analysis provides the highest resolution characterization accessible to most researchers.

In the example presented here, ceramic fragments from Bronze-age furnaces used for smelting metallic ores were analysed (materials provided by Prof. Aaron Shugar, Queen's University, Canada). These furnaces were employed in the initial stage of refining, where raw ore was mixed with materials such as sand and charcoal to produce a more concentrated metal material, which

could then be further refined in crucibles for metalworking. Much can be learned by examining the nature of a furnace wall fragment, including the method of furnace construction, firing temperatures, the level of smelting technology, and the origins of ores. This is achieved through the analysis of metal residues that may adhere as slag to, or transfer into, the furnace wall itself.

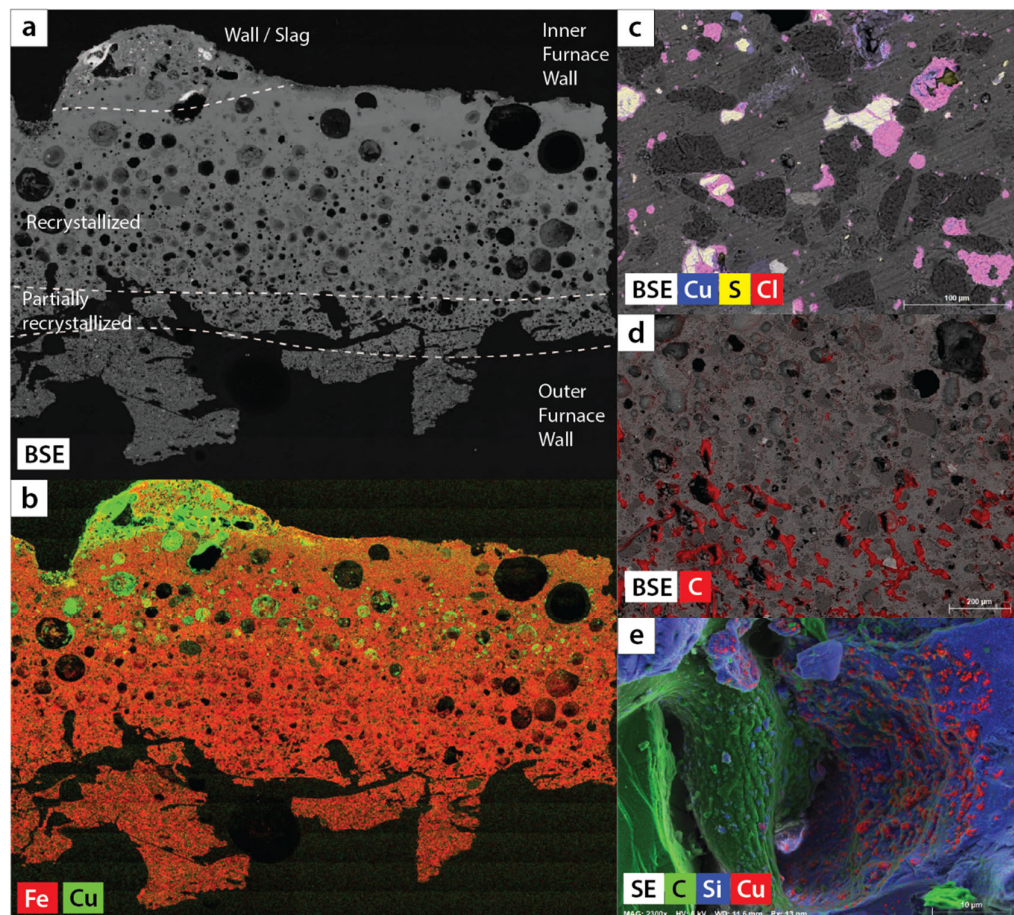


Figure 10. Bronze age furnace ceramic fragment examined by SEM-EDS. a) Backscattered electron (BSE) mosaic map of a fragment. The map is annotated to illustrate features described in the text. b) EDS mosaic map of a fragment showing the elemental distribution of Fe and Cu. c) Higher magnification elemental map overlay on BSE taken from the inner margins of the fragment (upper edge viewed in a)) showing the presence of copper minerals in the furnace wall. Note that copper sulphide minerals are being altered to copper chloride. d) Elemental map of carbon overlaid on the BSE map showing partial preservation of organic material in the ceramic. e) High-magnification secondary electron + elemental map of a pore space in the ceramic collected with an annular EDS detector.

Detailed analysis was conducted using an SEM equipped with a standard EDS detector (XFlash® Q80 compact EDS detector) with further investigation using an annular EDS detector (XFlash® FlatQUAD, Bruker Nano GmbH, Berlin). Image and point analysis across the furnace fragments

allowed access to information related to the key components of the original raw materials and the resulting fired ceramic. Backscatter electron (BSE) images with correlated EDS elemental maps (Figs. 10a to 10c) revealed the extent of copper penetration into the furnace wall, which was present as copper sulphide and copper chloride minerals. In addition, chemical and mineralogical zoning identified a transition from the outer to the inner furnace wall, which records a recrystallisation front related to the temperature gradient during furnace operation (Figs. 10a and 10b). Mineralogical transformations were only observed at the higher magnifications and smaller excitation volumes afforded by SEM analysis. With the light element capability of SEM-EDS analysis the boundary between partially and full recrystallised clay, where most organic material has been devolatilized and driven out, can be visualised, a record of a temperature gradient (Fig. 10d). Further, the ability to work with samples preserving some topography afforded by the annular detector, has allowed carbon residues that survived devolatilisation during firing to be imaged in pore spaces within the ceramic (Fig. 10e). Organic material, in the form of straw or other plant materials may be initially added to the furnace clay to provide support but also to stabilize the clay during firing by reducing cracking.

## 5. REFERENCES

- [ 1] Jaklevic M M, French W R, Clarkson T W and Greenwood M R 1978 *Adv. X-ray Anal.* **21** 171-185
- [ 2] Toribara T Y, Jackson D A, French W R, Thompson A C and Jaklevic J M 1982 *Anal. Chem.* **54** 1844-1849
- [ 3] Nichols M C, Boehme D R, Ryon R W, Wherry D, Cross B and Aden G 1987 *Adv. X-ray Anal.* **30** 45-51
- [ 4] Cross B J and Wherry D C 1987 *Adv. X-ray Anal.* **30** 39-44
- [ 5] Carpenter D A, Taylor M A and Holcombe C E 1989 *Adv. X-ray Anal.* **32** 115- 120
- [ 6] Carpenter D A and Taylor M A 1991 *Adv. X-ray Anal.* **34** 217-221
- [ 7] Nicolosi J A, Scruggs B and Haschke M 1998 *Adv. X-ray Anal.* **41** 19-25
- [ 8] Tagle R, *et al.* 2019 *A deeper insight into materials: Potentials and limitations of  $\mu$ -XRF*. in: Book of Tutorials and Abstracts of the EMAS 2019 - 16th European Workshop (19-23 May; Trondheim, Norway) [S. Mamede de Infesta, Portugal: EMAS]
- [ 9] Beckhoff B, Kanngießer B, Langhoff N, Wedell R, and Wolff H (Eds.) 2006 *Handbook of practical X-ray fluorescence analysis*. [Berlin-Heidelberg: Springer Verlag]
- [10] Scofield J H 1974 *Phys. Rev. A* **9** 1041
- [11] Salem S I, Panossian S L and Krause R A 1974 *Atom. Data Nucl. Data* **14** 91
- [12] Ertuğral B, Apaydın G, Çevik U, Ertuğral M and Koby A 2007 *Radiat. Phys. Chem.* **76** 15
- [13] Alberti R, *et al.* 2022 *J. Cult. Heritage* **58** 130-136
- [14] Vicenzi E P, *et al.* 2024 *Microsc. Microanal.* **30** (Suppl. 1) ozae044.055
- [15] Colomban P, *et al.* 2024 *Ceramics* **7** 1905-1929
- [16] Carpenter W (June 1986) *Metals suitable for enameling*. in: Glass on Metal – vol. 5, no. 6, June 1986. (Archived from the original on 5 February 2017; Retrieved 17 November 2007)